Phased Array Ghost Elimination (PAGE) for Segmented SSFP Imaging With Interrupted Steady-State

Peter Kellman[*], **Michael A. Guttman**, **Daniel A. Herzka**, and **Elliot R. McVeigh**
Laboratory of Cardiac Energetics, National Institutes of Health, National Heart, Lung and Blood Institute, Bethesda, Maryland.

Abstract

Steady-state free precession (SSFP) has recently proven to be valuable for cardiac imaging due to its high signal-to-noise ratio and blood-myocardium contrast. Data acquired using ECG-triggered, segmented sequences during the approach to steady-state, or return to steady-state after interruption, may have ghost artifacts due to periodic *k*-space distortion. Schemes involving several preparatory RF pulses have been proposed to restore steady-state, but these consume imaging time during early systole. Alternatively, the phased-array ghost elimination (PAGE) method may be used to remove ghost artifacts from the first several frames. PAGE was demonstrated for cardiac cine SSFP imaging with interrupted steady-state using a simple alpha/2 magnetization preparation and storage scheme and a spatial tagging preparation.

Keywords

FISP; SSFP; SENSE; ghost cancellation; myocardial tagging; cardiac imaging

---

Steady-state free precession (SSFP) (1) has recently proven to be valuable for cardiac imaging due to its high signal-to-noise ratio (SNR) and blood-myocardium contrast. Data acquired using ECG-triggered, segmented sequences during the approach to steady-state, or the return to steady-state after interruption, and disturbance due to magnetization preparation, may have ghost artifacts in the phase encode direction due to periodic *k*-space distortion. Schemes involving several preparatory RF pulses have been proposed to restore steady-state (2-4). For example, it is common to run a series of dummy alpha pulses prior to imaging (4) in order to discard signal acquired during the transient response, but this consumes imaging time during early systole, preventing the acquisition of early systolic cardiac phases. Pulse sequences may be designed to drive a tissue to steady-state (2,3), but their effectiveness has not been demonstrated in vivo. Alternatively, the phased-array ghost elimination (PAGE) (5) method may be used to remove ghost artifacts from the first several frames.

The interruption of the imaging steady-state may be necessary for magnetization preparation. For example, magnetization preparation such as spatial tagging or fat saturation require an interruption and restoration of the steady-state in order to be viable within SSFP imaging. For triggered cardiac cine images using a segmented *k*-space SSFP acquisition with interrupted steady-state, data acquired during the initial TRs (cardiac phases) have periodic variations in amplitude and phase which causes ghosting in the phase encode dimension. These variations are reduced for on-resonant species by the alpha/2 preparation scheme. However, ghosting

---

[*]Correspondence to: Peter Kellman, Laboratory of Cardiac Energetics, National Institutes of Health, National Heart, Lung and Blood Institute, 10 Center Drive, MSC-1061, Building 10, Room B1D416, Bethesda, MD 20892-1061. E-mail: kellman@nih.gov

remains due to off-resonance and other sources of error such as the RF excitation process, among others.

In this work, PAGE is demonstrated as a tool for the removal of ghosts in the context of cardiac cine SSFP imaging with interrupted steady-state using a simple alpha/2 preparation scheme. High temporal resolution spatial tagging is demonstrated as an example.

MATERIALS AND METHODS

Description and Theory

ECG-triggered cardiac cine images using a segmented *k*-space SSFP acquisition with interrupted steady-state were acquired using alpha/2 preparation pulses to reduce the transient approach to steady-state. The timing of the typical pulse sequence is diagrammed in Fig. 1. Optional RF magnetization preparations include tagging and fat saturation. The alpha/2 preparation pulse is played at time TR/2 before the first imaging alpha pulse and after the last imaging alpha pulse. Magnetization is effectively "stored" the along the z-axis by this last pulse, which reduces the amplitude and phase variations of the echoes when imaging is resumed after the next ECG trigger (6). Despite the alpha/2 preparation, initial cardiac phases exhibit significant ghosting particularly due to off-resonance effects. This is illustrated by the simulation shown in Fig. 2, which shows the amplitude and phase of the transverse magnetization component during the approach to steady-state for fat which is off-resonant due to chemical shift. In this example, the first heart beat has been discarded; succeeding heart beats behave almost identically. Simulations were based on the method described by Sekihara (7) and used the same imaging parameters described below. For a segmented *k*-space acquisition with four views-per-segment (VPS), the corresponding periodic *k*-space distortion gives rise to four ghosts as illustrated by the point spread functions (PSF) shown in Fig. 3 for the first eight cardiac phases. The PSFs were calculated by Fourier transform of the periodic *k*-space distortion. The PSF for the desired image without ghosts is at the center of the plot and 1/2 FOV ghosts are at the edge. The ghosts are largely due to phase modulation and, therefore, are not symmetric (i.e., the 1/4 FOV ghost amplitude does not equal the 3/4 FOV ghost amplitude). The total signal intensity of the ghosts decay during steady-state approach and the point spread function, i.e., the relative intensity of ghosts, is variable as well. For fat, steady-state is substantially achieved within several cardiac phases.

PAGE (5) may be used to cancel widely spaced ghosts in a manner similar to SENSE accelerated imaging (8). In the PAGE method, the superimposed images (ghosts) may be separated by phased array combining with appropriate weights, calculated by the inverse solution. In this application, we are considering the periodic variation in *k*-space weighting caused by the approach to steady-state. The superimposed images are weighted by $h_k(x,y)$ which will be referred to as a "point spread function" (PSF), even though it is understood that it is a function of (x,y) and, therefore, is actually space variant, due to spatial variation in tissue T_1, T_2, and off-resonance effects from chemical shift and field inhomogeneity

A block diagram of the signal processing steps for artifact cancellation described above is shown in Fig. 4. The sample images illustrate the case of $N_c = 4$ coils and four superimposed images spaced $D = FOV_y/4$. The individual component images, separated in this manner, are each weighted by complex PSF values $h_k(x,y,t)$, determined by the tissue parameters and off-resonance, as well as magnetization preparation. Root-sum-of-squares (RSS) magnitude combining was used for simplicity. The surface coil field maps (B_1-maps), $s_i(x,y)$, required for determining the phased array combiner coefficients were estimated from images for the later cardiac phases which were ghost-free. Ghost-free images were averaged and normalized by the RSS magnitude to obtain raw complex sensitivities with image modulus removed.

The inverse solution amplifies the noise, causing a loss in SNR which is spatially varying. The loss in SNR relative to the artifact free image is calculated as (5,8):

$$SNR_{loss} = \frac{1}{\sqrt{\left(S^H R_n^{-1} S\right)_{(1,1)}^{-1} \left(S^H R_n^{-1} S\right)_{(1,1)}}},$$

[1]

where the subscript (1,1) denotes the index of the matrix (first diagonal element). The spatially varying denominator of Eq. [1] is also referred to as the g-factor. Estimates of the g-factor were calculated from the sensitivities, **S**, and noise statistics, R_n, used in computing the unmixing matrix.

Experimental Parameters

All experiments were conducted using a GE Signa CV/*i* 1.5 T MR imaging system which was custom-modified for 8-channel operation using a multichannel digital receiver (9). Breathheld cine imaging of a single short axis slice was performed using an ECG-triggered, segmented acquisition of *k*-space over a number of heartbeats. Images were acquired using a Nova Medical (Wakefield, MA.) 8-element phased array, consisting of two linear arrays composed of four nonoverlapped, rectangular coils (21 × 5.25 cm with long dimension oriented along the superior-inferior direction), with one array positioned on the chest and the second array positioned on the back of the subject. Preamplifier decoupling was used to reduce mutual inductive coupling and additional isolation was achieved by capacitive nulling of the inductive coupling between adjacent elements. SSFP imaging was used with the following parameters: sequential phase-encode ordering, bandwidth ±125 kHz, TE = 1.6 msec, TR = 3.9 msec, 45° RF flip angle, and 8 mm slice thickness. Data was collected over approximately 75% of the cardiac cycle. Alpha/2 pulses (separated by TR/2 as shown in Fig. 1) were used at the beginning and end of each data collection period to accelerate the approach to steady-state and to store the magnetization, respectively. Each ECG-triggered imaging experiment began with one heartbeat of dummy RF pulses to achieve approximately the same beat-to-beat initial longitudinal magnetization for imaging. No dummy RF pulses were used during the imaging heartbeats. Image sets were alternately acquired with no further preparation and with grid tags (7-pixel spacing).

Studies were performed on five normal healthy volunteers. This protocol was approved by the Institutional Review Board of the National Heart, Lung, and Blood Institute. The FOV was typically 320 × 240 mm with an image matrix of 192 × 96, with corresponding in-plane spatial resolution approximately 1.7×2.5 mm^2. The 96 phase encodes were acquired using four views-per-segment (cardiac phase) during a breathhold period of 24 heartbeats. This resulted in a temporal resolution of 4 × TR = 15.6 ms, and 46 cardiac phases. The surface coil field maps (B_1-maps) were derived from an average of the last 26 cardiac phases which were ghost-free.

RESULTS

The first five cardiac phases are shown in Fig. 5 for a normal volunteer using various reconstructions. The rows correspond to cardiac phases with the first phase in the top row. Note that the ghost artifacts are greatest in the initial phases and disappear as steady-state is reached. The left column contains conventional RSS magnitude images and exhibits strong 1/4 and 1/2 FOV ghosts. The phased array (ghost cancelled) separated component images, desired image plus 1/4, 1/2, and 3/4 FOV ghosts, with h_0, h_1, h_2, and h_3 weightings are in columns 2-5, respectively. The right-most column contains the RSS combined magnitude ghost cancelled image.

Ghosting of the blood is predominately at 1/2 FOV and lasts several phases. Chest wall ghosts due to off-resonant fat are seen at 1/4, 1/2, and 3/4 FOV in the first cardiac phase and decay rapidly. The distribution of ghost varies considerably for different subjects and for different shimming.

Images comparing conventional magnitude reconstruction and ghost cancellation (PAGE) combined magnitude image for the first cardiac phase are shown in Fig. 6, left and right columns, respectively. The top row contains images without additional magnetization preparation; the bottom row contains images with grid tagging. A high degree of ghost artifact suppression is achieved. For example, the SNR of the LV blood pool artifact at 1/4 FOV for the first cardiac phase in Fig. 5 was measured to be greater than 50:1. This artifact is suppressed to the noise level or below.

PAGE causes a reduction in SNR by the SENSE g-factor. The g-factors are highly variable across the FOV. In this example, with specific eight-coil array, coil placement, and slice orientation, the g-factor was measured to be as high as 2.6 (worst case in the region-of-interest). This value is consistent with theoretical predictions for this array, which has been simulated for a range of parameters including FOV and slice orientation. Maximum values for the g-factor in the region-of-interest ranged from 2.0-3.0 for different subjects and slice orientations. Using the standard GE product four-coil phased array the worst case g-factors were measured to be in the range of 4-5, causing SNR loss and increased sensitivity to B_1-map errors due to ill-conditioning.

DISCUSSION

The SNR penalty using the PAGE method with eight coils to cancel four ghosts, corresponding to segmented acquisition with four views per segment, is moderate, although the SNR loss from PAGE is somewhat offset by the fact that initial phases typically have higher SNR due to regrowth of the longitudinal magnetization before the ECG trigger. Nevertheless, even with this reduction in SNR, the first few cardiac phases have excellent quality. The g-factor-related SNR loss for applications with a greater number of ghosts, corresponding to a higher number of views per segment, would be significantly higher even using eight receiver coils. An important application for this method is high temporal resolution analysis of heart function using tagging, which requires the initial phases following the tagging pulse. For the ghost-free images in the later cardiac phases, conventional reconstruction may be used, thereby avoiding the SNR penalty entirely. In this case, B_1-weighted phased array combining may be used (with the same B_1-maps used for calculating the unmixing coefficients) in order to avoid intensity variation between the PAGE and non-PAGE processed images.

CONCLUSION

We have demonstrated the use of PAGE in removal of ghost artifacts from SSFP images acquired during the approach to steady-state. This application is particularly important for situations requiring interruption of the steady-state, such as high temporal resolution SSFP imaging with tagging. Using PAGE with simple alpha/2 RF preparation, the ghosts are cancelled without resorting to more time-consuming RF preparation schemes and the initial image frames immediately after tagging, which would otherwise be discarded, may now be used.

The PAGE method is limited in the number of ghosts that can be cancelled due to the loss in SNR incurred due to ill-conditioning (SENSE g-factor), which depends on the number and geometry of surface coils. Using eight-coil reception a practical limit of four ghosts is reached, corresponding to four views-per-segment with a sequential phase encode order and a net SNR

loss of approximately 2:1, including g-factor losses and magnetization regrowth during the trigger window.

REFERENCES

1. Oppelt A, Graumann R, Barfuss H, Fischer H, Hartl W, Schajor W. FISP: eine neue schnelle Pulssequenz fur die Kernspintomographie. Electromedica 1986;54:15–18.

2. Deimling, M.; Heid, O. Magnetization prepared true FISP imaging; Proc 2nd Annual Meeting SMRM; San Francisco. 1994; p. 495

3. Hargreaves BA, Vasanawala SS, Pauly JM, Nishimura DG. Characterization and reduction of the transient response in steady-state MR imaging. Magn Reson Med 2001;46:149–158. [PubMed: 11443721]

4. Deshpande VS, Shea SM, Laub G, Simonetti OP, Finn JP, Li D. 3D magnetization-prepared true-FISP: a new technique for imaging coronary arteries. Magn Reson Med 2001;46:494–502. [PubMed: 11550241]

5. Kellman P, McVeigh ER. Ghost artifact cancellation using phased array processing. Magn Reson Med 2001;46:335–343. [PubMed: 11477638]

6. Scheffler K, Heid O, Hennig J. Magnetization preparation during the steady state: fat-saturated 3D TrueFISP. Magn Reson Med 2001;45:1075–1080. [PubMed: 11378886]

7. Sekihara K. Steady-state magnetizations in rapid NMR imaging using small flip angles and short repetition intervals. IEEE Trans Med Imag 1987;6:157–164.

8. Pruessmann KP, Weiger M, Scheidegger MB, Boesiger P. SENSE: sensitivity encoding for fast MRI. Magn Reson Med 1999;42:952–962. [PubMed: 10542355]

9. Morris, HD.; Derbyshire, JA.; Kellman, P.; Chesnick, AS.; Guttman, MA.; McVeigh, ER. A wide-bandwidth multi-channel digital receiver and realtime reconstruction engine for use with a clinical MR scanner; Proc 10th Scientific Meeting ISMRM; Honolulu. 2002; p. 61
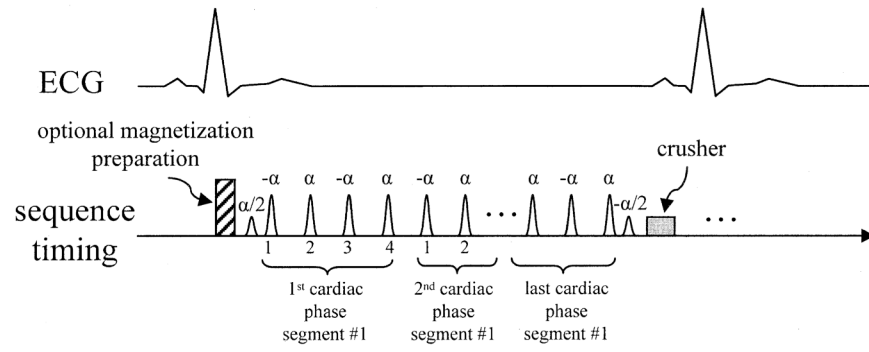
FIG. 1.
Timing of pulse sequence for ECG triggered segmented SSFP acquisition with optional magnetization preparation including fat saturation or spatial tagging. Alpha/2 pulses are played TR/2 from the first and last alpha pulses. In this example, four phase encode lines from each segment are grouped into a cardiac phase.
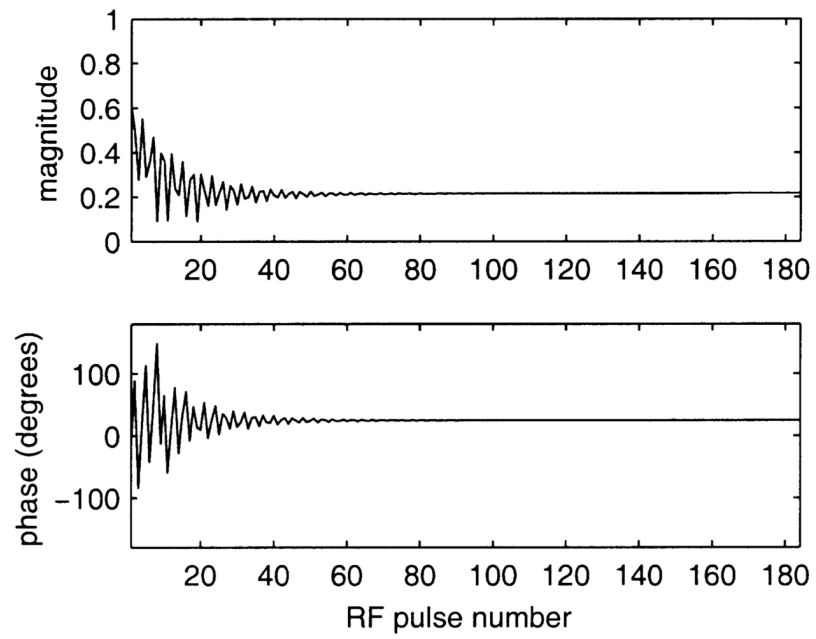
FIG. 2.
Example of simulated approach to steady-state for fat using ECG triggering and simple alpha/
2 preparation scheme, shown for a single heartbeat (first heartbeat has been discarded).
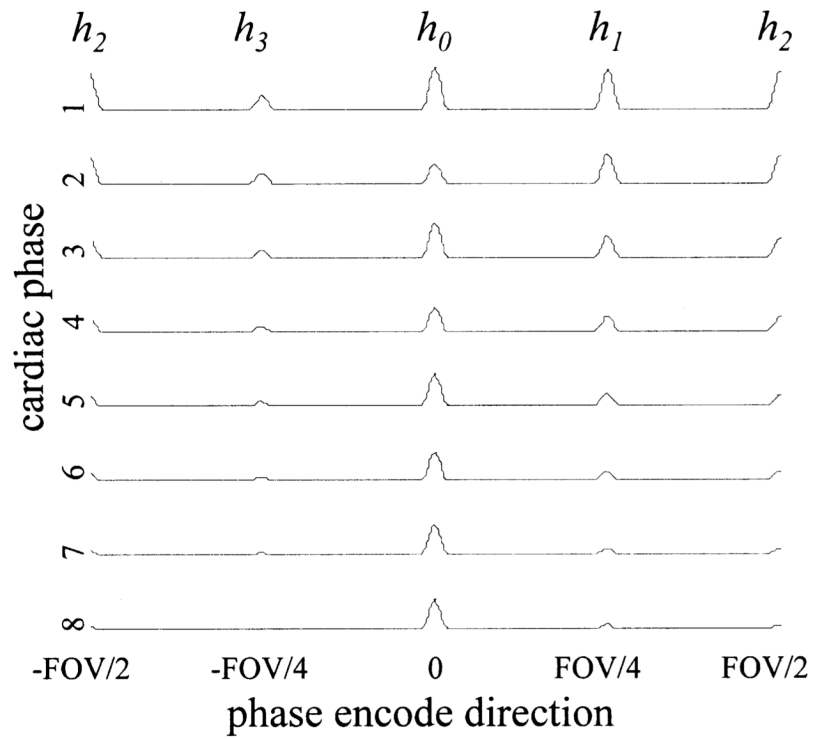
FIG. 3.
Example of simulated point spread functions for fat illustrating ghosts during approach to steady-state. Ghosts at ±1/4 and ±1/2 FOV fade as the transient response subsides.
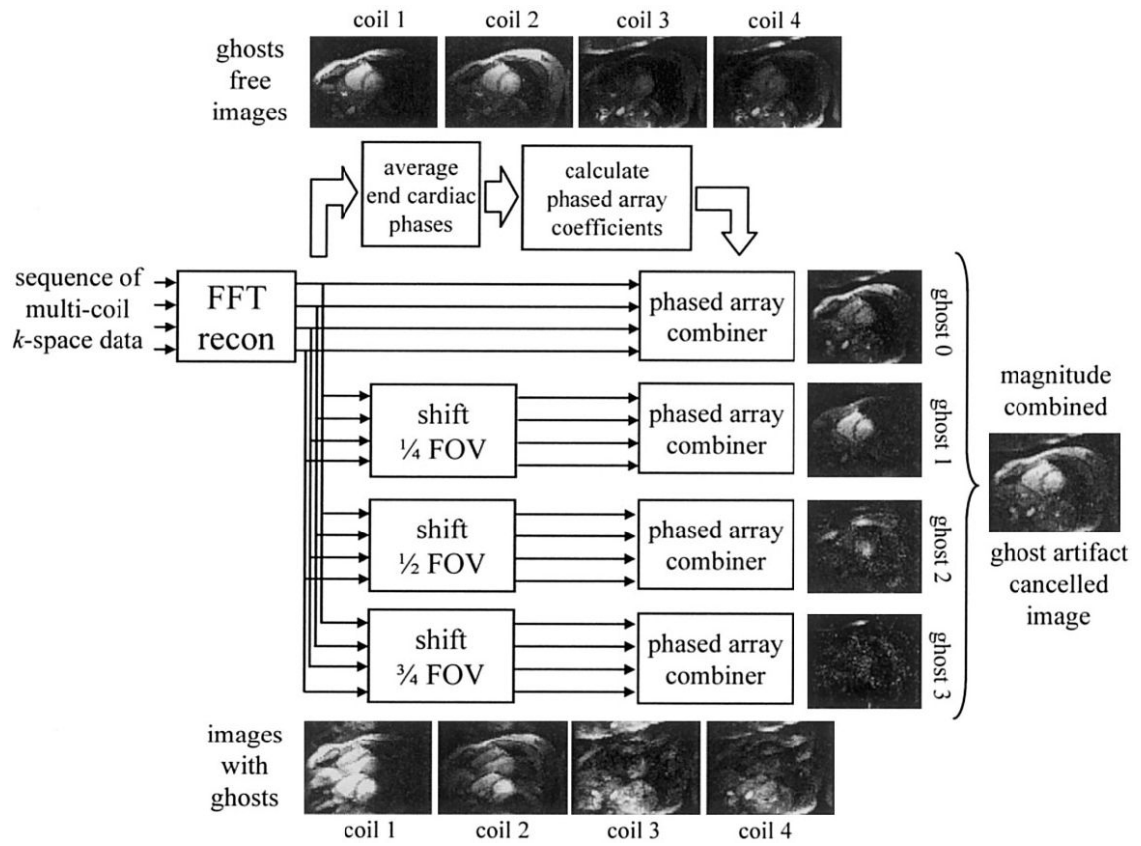
FIG. 4.
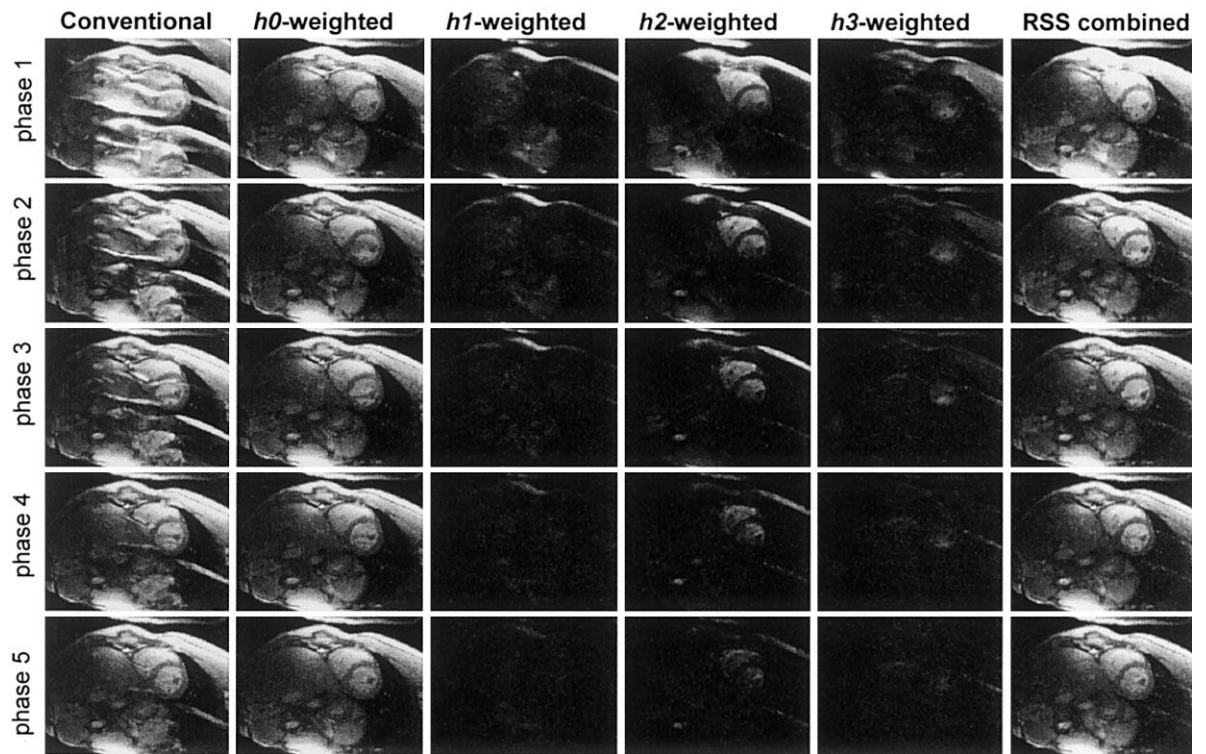Block diagram of PAGE method applied to interrupted steady-state segmented SSFP.

FIG. 5.
Images comparing conventional image reconstruction with ghosts (left column) and PAGE reconstructed images (right columns) for ECG triggering segmented SSFP acquisition during initial cardiac phases (no magnetization preparation). The individual separated ghost image components are shown in columns 2-5. The ghost-cancelled RSS combined magnitude images (excluding h_3-weighted images of column 5) are shown in right the column.

Conventional

Ghost Cancelled
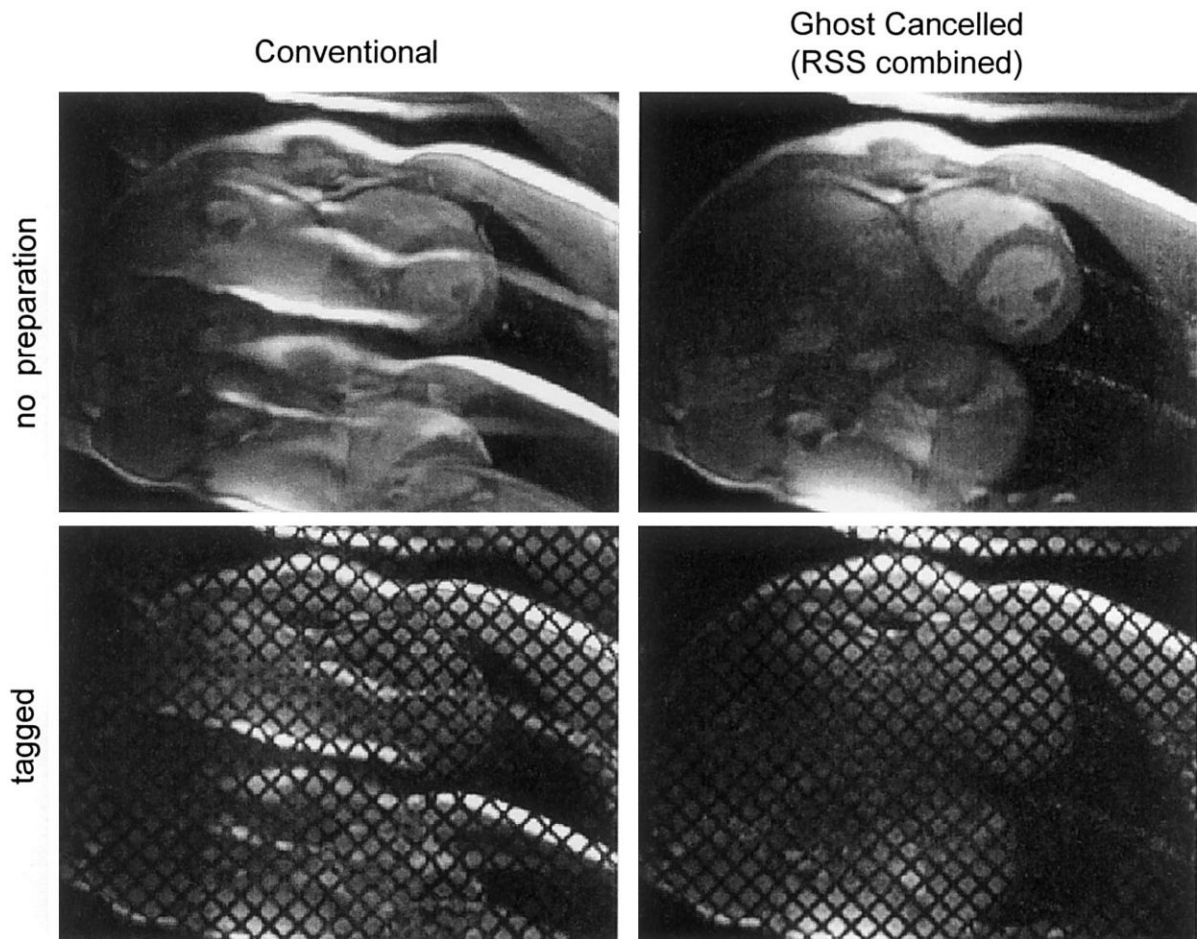(RSS combined)

no preparation

tagged

FIG. 6.
Images for first cardiac phase comparing conventional image reconstruction with ghosts (left column) and PAGE-reconstructed images (right column) for ECG triggering segmented SSFP acquisition with no magnetization preparation (top row) and tagging (bottom row).